

Experimental charge-density study of paracetamol – multipole refinement in the presence of a disordered methyl group

Joanna M. Bąk,^a Paulina M. Dominiak,^a Chick C. Wilson^b and Krzysztof Woźniak^{a*}^aChemistry Department, Warsaw University, 02-093 Warszawa, Pasteura 1, Poland, and^bDepartment of Chemistry, University of Glasgow, Glasgow G12 8QQ, UK. Correspondence e-mail: kwozniak@chem.uw.edu.pl

A high-resolution single-crystal X-ray study of paracetamol has been performed at 85 K. Different approaches to modeling the experimental electron density (ED) were tested for the dynamically disordered portions of the molecule in order to check to what extent it is possible to obtain a proper ED distribution in the ordered part. Models were examined in which the methyl-group ED was built from pseudoatoms taken from the University at Buffalo Pseudoatom Databank or the Invariom database, with multipole parameters for the remaining atoms being obtained from free refinement. The κ' restricted multipolar model (KRMM) and free κ' refinements were compared; restriction of the κ' parameters was essential in order to obtain values of the electrostatic interaction energy consistent with the results of theoretical single-point periodic calculations. After simultaneous use of KRMM refinement and the databases to model the methyl group, the bond critical point properties and interaction electrostatic energy values were found to be closer to those obtained from theory. Additionally, some discrepancies in the ED distribution and dipole moment among transferred aspherical atom model refinements utilizing both theoretical databases and parameters from theoretical periodic calculations are shown. Including the influence of the crystal field in the periodic calculations increases the ED in the hydroxyl and amide groups, thus leading to higher values of the electrostatic interaction energy, changes in the electrostatic potential values mapped on the isodensity surface and changes in the shape of the anisotropic displacement parameters with respect to results found for both database models.

© 2009 International Union of Crystallography
Printed in Singapore – all rights reserved

1. Introduction

Paracetamol (*p*-hydroxyacetanilide; see Fig. 1) is an important bioactive compound. It has been intensively studied in the crystalline state. Several polymorphs have been characterized (Haisa *et al.*, 1974, 1976; Boldyreva *et al.*, 2000). The monoclinic form was found to be the most thermodynamically stable (Haisa *et al.*, 1976) and for this form temperature-dependent neutron diffraction experiments (Wilson, 1997) and periodic quantum-chemical calculations (Johnson *et al.*, 1999; Binev *et al.*, 1998) have been performed. The studies show that the terminal methyl group of the compound displays tunneling dynamic disorder (Wilson, 1997) and the electron-density distribution in this group is sensitive to intermolecular hydrogen bonding (Johnson *et al.*, 1999). The presence of disorder is a challenging problem in high-resolution electron-density (ED) studies. In a recent attempt to carry out an ED study of molecules containing disorder, the rotational disorder of methyl 2-aminoisobutyrate hydrochloride (Dittrich *et al.*,

2009) was qualitatively characterized by a difference density approach. Disordered non-H atoms of cyclosporine A were modeled using the Gram–Charlier expansion up to the third order, and static disorder of H atoms was refined in the charge-density study of Johnas *et al.* (2009). Proper modeling of disorder is an important topic, as disordered groups are frequently found in large biological molecules. Therefore, we have decided to perform a high-resolution X-ray diffraction study of paracetamol crystals in order to check to what extent it is possible to obtain a reasonable ED for a molecule of this type containing dynamic disorder. Prior to our carrying out this work, no experimental charge density of paracetamol had been published. [A paper by Bouhmaida *et al.* (2009) was published at nearly the same time as the present paper was submitted; disorder of the methyl group is not mentioned in Bouhmaida *et al.* (2009).]

The model of the ED most frequently used in multipole refinements is based on the Hansen & Coppens formalism (Hansen & Coppens, 1978), which describes the static ED by a

superposition of aspherical pseudoatoms represented by atom-centered density expansions,

$$\rho^{\text{atom}}(\mathbf{r}) = P_c \rho^{\text{core}}(\mathbf{r}) + P_v \kappa^3 \rho^{\text{valence}}(\kappa r) + \sum_{l=0}^{l(\text{max})} \kappa'^3 R_l(\kappa' \zeta r) \sum_{m=0}^l \sum_p P_{lmp} d_{lmp}(\theta, \varphi).$$

The atomic scattering factor is calculated from the Fourier transform of the pseudoatomic density. The core population P_c is kept unrefined and the pseudoatom parameters (contraction–expansion coefficients κ and κ' , along with the populations P_v and P_{lmp}) are refined in the least-squares fitting procedure against experimental structure factors. ρ^{core} and ρ^{valence} represent the core and valence normalized Hartree–Fock density functions of the free atom, and R_l and d_{lmp} are the radial and spherical harmonics functions, respectively. The mathematical expression of thermal motion and the Fourier transform of multipolar expansion are strongly convoluted (Coppens, 2006). Hence, reliable information about the ED distribution can be obtained only when atomic positions and thermal motion are defined accurately and the X-ray diffraction data are collected to the highest possible resolution (Koritsanszky & Coppens, 2001; Madsen *et al.*, 2004).

Proper deconvolution of thermal motion and bonding density strongly depends on the refinement strategy and might be achieved by several approaches. Precise positions and anisotropic displacement parameters (ADPs) of all atoms can be obtained from neutron diffraction data, but these are not always available. High-order refinement, performed against

high-resolution X-ray diffraction data (typically $\sin \theta/\lambda > 0.8 \text{ \AA}^{-1}$), can lead to reasonable coordinates and ADPs for the non-H atoms. In cases where high-quality neutron data are not available, the ADPs for the H atoms can also be estimated using a combination of a TLS fit with internal contributions from high-quality neutron studies of related materials (Madsen, 2006). Other methods for estimating H-atom ADPs have been proposed (Whitten & Spackman, 2006; Flaig *et al.*, 1998; Roversi & Destro, 2004).

Brock *et al.* (1991) introduced the idea of transferability of pseudoatom parameters in the Hansen–Coppens model between different molecules, initiating the creation of databanks of aspherical atom parameters. There are three databanks: the experimental ELMAM database (Pichon-Pesme *et al.*, 1995, 2004; Domagała & Jelsch, 2008), the theoretical Invariom database (Dittrich *et al.*, 2004; Dittrich, Hübschle *et al.*, 2006) and the University at Buffalo Pseudoatom Databank (UBDB) (Volkov, Li *et al.*, 2004; Dominiak *et al.*, 2007). With these databases it is possible to model ED and accurately deconvolute thermal motion within the transferred aspherical atom model (TAAM) refinement (Volkov *et al.*, 2007; Dittrich *et al.*, 2008; Pichon-Pesme *et al.*, 1995). In such a refinement, pseudoatom parameters for each species are transferred from the chosen database and only coordinates and ADPs are refined. It is already known that the TAAM refinement significantly improves the discrepancy R factors, molecular geometry (Dittrich *et al.*, 2007; Volkov *et al.*, 2007; Dittrich, Hübschle *et al.*, 2006; Jelsch *et al.*, 2005) and precision of the Flack parameter (Dittrich, Strumpel *et al.*, 2006) with respect to the independent atom model (IAM). It also leads to ADPs closer to those obtained from multipole refinements (Volkov *et al.*, 2007; Dittrich *et al.*, 2008).

The advantages and disadvantages of experimental *versus* theoretical databases have been discussed by Pichon-Pesme *et al.* (2004) and Volkov, Koritsanszky *et al.* (2004). The major advantages of theoretical databases are the absence of experimental error in the construction process and the availability of unlimited types of pseudoatoms. The procedures of atom type recognition and databank construction differ between the Invariom and UBDB approaches. In the UBDB method, each atom type results from averaging over a family of chemically unique pseudoatoms derived from the theoretical densities of a number of small molecules. The theoretical densities are obtained from B3LYP/6-31G** single-point calculations on the basis of experimental geometries taken from the CSD (Allen, 2002). In the Invariom database each pseudoatom is derived from a unique model compound. The B3LYP/D95++(3df,3pd) basis set is used to optimize the geometry and generate the density of the model compound. Another difference is that in the UBDB method the valence-only structure factors are used and the core electrons are added after the fitting procedure, whereas in the Invariom approach the structure factors are obtained from the Fourier transform of all (valence and core) orbitals. In both databases the influence of the crystal field on the charge-density distribution is not taken into account; one possibility for overcoming this limitation is to use modern periodic calculations

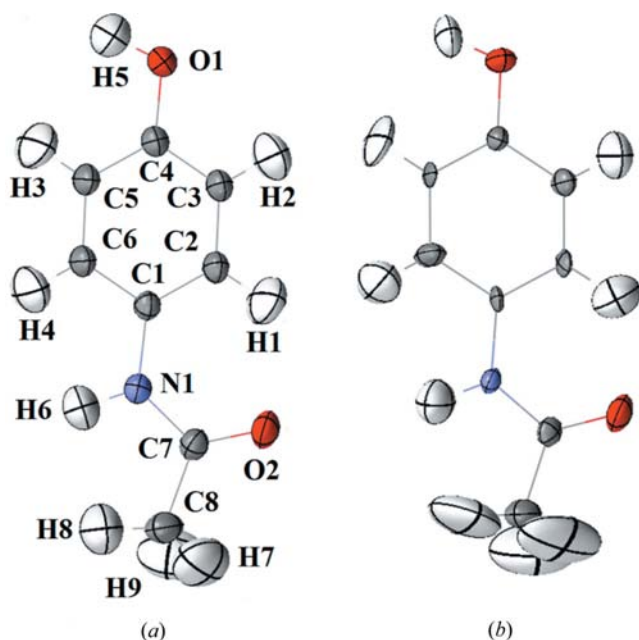


Figure 1 Structure of paracetamol: (a) anisotropic displacement parameters (ADPs) at the 90% probability level for non-H atoms after high-order refinement against X-ray diffraction data (85 K) and for H atoms generated by the *SHADE* program; (b) ADPs at the 90% probability level from neutron diffraction data (80 K; Wilson, 1997).

(Pisani *et al.*, 1988; Spackman & Mitchell, 2001; Munshi & Guru Row, 2006).

In this work, we study the influence of the disordered methyl group on the multipolar description of the ED in the whole molecule, to see whether this influence is revealed in other parts of the molecule as described by Dittrich *et al.* (2009) for methyl 2-aminoisobutyrate hydrochloride. We aim to check whether it is possible to perform free multipole refinement for the ordered part of the molecule when the ED in the disordered part (the methyl group) is modeled by pseudoatoms from the UBDB (Dominiak *et al.*, 2007) or the Invariom database (Dittrich, Hübschle *et al.*, 2006). By comparing free multipole refinement, kappa-restricted multipole refinement, multipole refinements with a restricted methyl group, and TAAM refinements with both theoretical databases and theoretical periodic calculations, it will be possible to identify some limitations of the above models and their influence on the ED topological properties, the electrostatic energies of interactions, the dipole moment and the ADPs of paracetamol.

2. Experimental

Single crystals of paracetamol (*p*-hydroxyacetanilide; purchased from Sigma Aldrich) were grown by evaporation of ethanol–aqueous solution. High-resolution X-ray diffraction measurements were carried out on a Bruker AXS KAPPA APEX II ULTRA diffractometer with a TXS rotating molybdenum anode and multilayer optics at a temperature of 85 K. Data were collected using the ω -scan method, with a scan width of 0.3° and a minimal and maximal exposure time of 10 and 50 s per frame, respectively. The data were corrected for Lorentz and polarization effects. Indexing, integration and scaling were performed with the Bruker *APEX-II* software supplied (Bruker Nonius, 2007). A multi-scan absorption correction was applied using *SADABS-2004/1, 2007* (Sheldrick, 1996). Crystallographic data are given in Table 1.

3. Calculation of periodic wavefunction and theoretical structure factors

Single-point periodic calculations were performed using the *CRYSTAL06* program (Dovesi *et al.*, 2008). Two modified 80 K neutron geometries of paracetamol were tested (one with the methyl H atoms shifted to the standard neutron distance of 1.059 Å and the other with the H atoms shifted to a distance of 1.09 Å, corresponding to the assumptions made in the Invariom database) and compared with the calculations performed for 20 K neutron geometry (where the disorder is less pronounced). The density functional theory (DFT) method at the B3LYP (Becke, 1993; Lee *et al.*, 1988) level with the 6-31G** basis set (Hariharan & Pople, 1973) was applied. This basis set has recently been shown to provide reliable and consistent results in studies involving intermolecular interactions (Munshi & Guru Row, 2006; Oddershede & Larsen, 2004). The shrinking factors (IS) along the reciprocal-lattice vectors were set at 4 (30 *k* points in the irreducible Brillouin

Table 1
Experimental details.

Chemical formula	C ₈ H ₉ NO ₂
Measurement temperature (K)	85
Wavelength (Å)	0.71073
Crystal system, space group	Monoclinic, <i>P</i> ₂ ₁ / <i>n</i>
<i>a</i> , <i>b</i> , <i>c</i> (Å)	7.077 (2), 9.173 (2), 11.574 (4)
β (°)	97.90 (2)
<i>V</i> (Å ³)	744.2 (4)
<i>Z</i>	4
No. of measured, independent and observed [<i>F</i> > 3 σ (<i>F</i>)] reflections	46012, 8661, 6967
<i>R</i> _{int} , <i>R</i> _{σ}	0.021, 0.016
Average <i>I</i> / σ (<i>I</i>)	35.94
μ (mm ⁻¹)	0.10
<i>T</i> _{min} / <i>T</i> _{max}	0.9207/1.0000
(<i>sin</i> θ / λ) _{max} (Å ⁻¹)	1.11
Index ranges	<i>h</i> : -14 to 15 <i>k</i> : -20 to 19 <i>l</i> : -25 to 19

zone). The truncation parameters were set as ITOL1–ITOL4 = 6 and ITOL5 = 15. The exponents of the polarization functions were not scaled due to a large difference between ITOL4 and ITOL5, as suggested by Spackman & Mitchell (2001). The level shifter value was set to 0.5 Hartree. Upon energy convergence the periodic wavefunctions were obtained and used to generate static theoretical structure factors up to a resolution of $\sin \theta/\lambda = 1.1 \text{ \AA}^{-1}$ using the XFAC command in *CRYSTAL06*.

4. Multipole refinements

Multipole refinements on $|F|$ were performed with the *XDLSM* program of the *XD2006* package (Volkov *et al.*, 2006). In all refinements atomic positions from neutron diffraction data were used as a starting point (Wilson, 1997). The set of refined parameters was gradually increased in the following order (Hoser *et al.*, 2009): (1) scale factor; (2) positions and ADPs for non-H atoms in a high-order refinement ($\sin \theta/\lambda > 0.8 \text{ \AA}^{-1}$), then the coordinates and ADPs were fixed until the final cycles of the refinements; (3) valence populations; (4) all dipoles for non-H atoms and bond-directed dipoles for H atoms; (5) quadrupoles for non-H atoms and bond-directed quadrupoles for H atoms; (6) octupoles for non-H atoms; (7) hexadecapoles for non-H atoms; (8) κ for non-H atoms; (9) positions and ADPs for non-H atoms.

The details of the particular refinement procedures carried out here, all following the general scheme outlined above, are defined as:

(1) *M*. After high-order refinement of positions and ADPs for non-H atoms, the methyl H atoms (H7, H8, H9) were shifted to the standard neutron *X*–H distance of 1.059 Å (Allen *et al.*, 1987), whereas for the remaining H atoms their positions from neutron diffraction data were retained. Next, the ADPs for H atoms were generated by the *SHADE* program (Simple Hydrogen Anisotropic Displacement Estimator) (Madsen, 2006). Generally, the ADPs for H atoms from neutron diffraction are the best choice for experimental

charge-density studies. However, where disorder is present, as in this case, the application of ADPs taken from neutron experiments to the methyl H atoms led to extremely high values of ρ at the bond critical points. Therefore we decided to use ADPs generated by *SHADE*. In the ordered part of the molecule, the use of ADPs generated by *SHADE* led to better residual maps derived from charge-density models than the problematic neutron ADPs (see Fig. 1, e.g. C1, C5 and H3). κ and κ' were freely refined after refinement of multipole populations. κ and κ' for C atoms were divided into five groups: three aromatic ones, one methyl group and one amino-acid group; κ and κ' for H atoms were fixed at a value of 1.2.

(2) *M_IDP(H)*. After high-order refinement of positions and ADPs for non-H atoms, a low-order ($\sin \theta/\lambda < 0.8 \text{ \AA}^{-1}$) refinement was performed to find the best positions and isotropic displacement parameters for H atoms. After that, all H atoms were shifted to the standard neutron $X-H$ distances (Allen *et al.*, 1987) and their positions fixed. κ and κ' were freely refined after refinement of multipole populations. κ and κ' for C atoms were divided into five groups: three aromatic ones, one methyl group and one amino-acid group. κ and κ' for H atoms were fixed at a value of 1.2.

(3) *M_UB*. A procedure similar to *M* was used with the following exceptions: P_v , P_{imp} , κ and κ' for the methyl-group atoms (C8, H7, H8, H9) were transferred from the UBDB (Dominiak *et al.*, 2007) and kept unrefined. κ and κ' for H atoms were divided into two groups: the methyl group and others. κ and κ' for the atoms from the methyl group were fixed at the values from the UBDB database.

(4) *M_IM*. A procedure similar to *M* was used with the following exceptions: P_v , P_{imp} , κ and κ' for the methyl-group atoms (C8, H7, H8, H9) were transferred from the Invariom database (Dittrich, Hübschle *et al.*, 2006) and kept unrefined; methyl H atoms were shifted to the theoretical C–H distance of 1.09 Å as recommended in Dittrich, Hübschle *et al.* (2006). κ and κ' for H atoms were divided into two groups: the methyl group and others. κ and κ' for the atoms from the methyl group were fixed at the values from the Invariom database.

(5) *M_KRMM*. A procedure similar to *M* was used but KRMM refinement was performed with constrained averaged κ' parameters from theoretical calculations (Volkov *et al.*, 2001), therefore κ and κ' for H atoms were also fixed, at values of 1.13 and 1.29, respectively.

(6) *M_UB_KRMM*. A procedure similar to *M_KRMM* was used with the following exceptions: P_v , P_{imp} , κ and κ' for the methyl-group atoms (C8, H7, H8, H9) were transferred from the UBDB (version 10 October 2006; Dominiak *et al.*, 2007) and kept unrefined. κ and κ' for H atoms were divided into two groups: the methyl group and others. κ and κ' for the atoms from the methyl group were fixed at the values from the UBDB database.

(7) *M_IM_KRMM*. A procedure similar to *M_KRMM* was used with the following exceptions: P_v , P_{imp} , κ and κ' for the methyl-group atoms (C8, H7, H8, H9) were transferred from the Invariom database (version DABA; Dittrich, Hübschle *et al.*, 2006) and kept unrefined; methyl H atoms were shifted to the theoretical C–H distance of 1.09 Å as recommended in

Table 2

Aspherical atom types assigned from the Invariom and UBDB databases.

For Invariom, the *Invariomtool* program (Hübschle *et al.*, 2007) was used. For the UBDB database *LSDB* (version 10 October 2006; Volkov, Li *et al.*, 2004) was used.

Atom label	Invariom atom type	UBDB atom type
C1	C1.5c[1.5c1h]1.5c[1.5c1h]1n	C354
C2, C3, C5, C6	C1.5c[1.5c1n]1.5c[1.5c1h]1h	C351
C4	C1.5c[1.5c1h]1.5c[1.5c1h]1o	C355
C7	C1.5o1.5n[1c1h]1c	C304
C8	C1c1h1h1h	C402
N1	N1.5c[1.5o1c]1c1h	N312
O1	O1c1h	O204
O2	O1.5c[1.5n1c]	O104
H1, H2, H3, H4	H1c[1.5c1.5c]	H104
H5	H1o[1c]	H111
H6	H1n[1.5c1c]	H107
H7, H8, H9	H1c[1c1h1h]	H101

Dittrich, Hübschle *et al.* (2006). κ and κ' for H atoms were divided into two groups: the methyl group and others. κ and κ' for the atoms from the methyl group were fixed at the values from the Invariom database.

THEOR. Several multipole refinements were performed against theoretical structure factors of all geometries (80 K, $d_{C-H} = 1.059 \text{ \AA}$; 80 K, $d_{C-H} = 1.09 \text{ \AA}$; 20 K). Multipoles up to hexadecapolar level were allowed to refine with individual κ and κ' parameters for each non-H atom. The atomic positions were not refined. Two approaches to H-atom refinement were tested: (a) 'UBDB-like' with bond-directed multipoles up to quadrupole and $\kappa = \kappa'$ parameters refined (Whitten *et al.*, 2006) and (b) 'Invariom-like' with bond-directed multipoles up to hexadecapole and κ parameters refined, and κ' parameters set to 1.2 and kept unrefined. For the latter, the refinements converged and gave consistent results for 80 K geometry ($d_{C-H} = 1.091 \text{ \AA}$) and 20 K geometry (see Table 1S in the supplementary material¹). Therefore, we chose as a reference 80 K geometry with a methyl C–H bond length of 1.091 Å (marked as THEOR).

TAAM. Transferred aspherical atom model (TAAM) refinements of positions and ADPs were carried out using *XDLSM*. TAAM refinements were performed in the following way: (1) structures were solved and refined by the IAM method in *SHELX* (Sheldrick, 2008; data cutoff $\sin \theta/\lambda < 0.7 \text{ \AA}^{-1}$); (2) scale factor and structure refinement were repeated in *XDLSM* against low-resolution data ($\sin \theta/\lambda < 0.7 \text{ \AA}^{-1}$); (3) P_v , P_{imp} , κ and κ' parameters were taken from the Invariom database (Dittrich, Hübschle *et al.*, 2006) (marked as TAAM_IM) or the UBDB database (Dominiak *et al.*, 2007) (marked as TAAM_UB), parameters were kept unrefined; (4) H atoms were shifted along experimental $X-H$ directions to the values recommended by the particular database; positions and ADPs for non-H atoms and isotropic displacement parameters for H atoms were refined in *XDLSM* against all

¹ Supplementary material for this article is available from the IUCr electronic archives (Reference: CN5019). Services for accessing this material are described at the back of the journal.

data. Details of the pseudoatoms used are listed in Table 2. TAAM_TH refinement (following the procedure described above) of positions and ADPs for non-H atoms and isotropic displacement parameters for H atoms, with density parameters taken from THEOR, was also performed against experimental data.

5. Results and discussion

The results of the refinements are summarized in Table 3. All statistics, *i.e.* $R(F)$, $wR(F)$, goodness of fit and residual densities, are comparable for models where multipole parameters were refined [M_IDP(H), M, M_UB, M_IM, M_{KRMM}, M_UB_{KRMM} and M_IM_{KRMM}]. The statistics are slightly worse for TAAM refinements (TAAM_TH, TAAM_UB and TAAM_IM), but still much better than for the IAM refinement, the R factor being lower by about 0.01. A similar decrease of the R factor was observed in previous studies concerning the application of the UBDB (Volkov *et al.*, 2007), the Invariom database (Dittrich, Hübschle *et al.*, 2006; Dittrich *et al.*, 2005) and the experimental ELMAM databank (Jelsch *et al.*, 2005).

Residual maps for all the refinements are given in Fig. 1S in the supplementary material. Although residual maps from the M, M_{KRMM} and M_IDP(H) refinements seem to be flat, we suspect that the static ED from these refinements is not properly deconvoluted from atomic motion, especially in the methyl-group region. Therefore, the M_UB, M_IM, M_UB_{KRMM} and M_IM_{KRMM} refinements with the ED for the methyl-group atoms transferred from the given database were performed and compared with the results from TAAM refinements and theoretical calculations. To point out the advantages and limitations of the models we focused on the following properties: the electron density and Laplacian values at the bond critical points (BCPs), the electrostatic energies of interaction, the dipole moment, the distribution of the electron density and the shape of the ADPs.

5.1. Electron density $\rho(\text{BCP})$ and Laplacian $\Delta\rho(\text{BCP})$ at bond critical points

Application of multipole parameters from the databases to model the methyl group (M_UB, M_IM, M_UB_{KRMM} and M_IM_{KRMM}) increases the values of $\rho(\text{BCP})$ and $|\Delta\rho(\text{BCP})|$ at the methyl C–H bonds with respect to the M and M_{KRMM} refinements (Fig. 2 and Fig. 3S in the supplementary material). This is mainly because of an inadequate description of the methyl-group disorder in the M and M_{KRMM} models, since the estimated ADPs are too compact in these models. On the other hand, the application of ADPs taken from the neutron experiment, with elongated ellipsoids, leads to values of these properties which are too high (data not shown). Considering the M_IM, M_IM_{KRMM} and M_UB, M_UB_{KRMM} refinements, the latter two give higher values of $\rho(\text{BCP})$ and $|\Delta\rho(\text{BCP})|$, which is mostly due to the different C–H distances applied.

Table 3
Refinement statistics.

Statistics were calculated for high-resolution data $[(\sin \theta/\lambda)_{\max} = 1.1 \text{ \AA}^{-1}]$.

Model	$R(F)$	$wR(F)$	Goodness of fit	Maximum and minimum residual density (e \AA^{-3})	
IAM	0.031	0.042	4.97	−0.21, 0.63	
Multipole model	M_IDP(H)	0.016	0.015	1.93	−0.13, 0.14
	M	0.015	0.015	1.86	−0.12, 0.13
	M _{KRMM}	0.015	0.015	1.89	−0.14, 0.14
	M_UB	0.017	0.016	2.02	−0.20, 0.26
	M_IM	0.017	0.016	2.05	−0.20, 0.26
	M_UB _{KRMM}	0.017	0.016	2.02	−0.22, 0.29
	M_IM _{KRMM}	0.017	0.017	2.07	−0.20, 0.27
TAAM	TAAM_TH	0.018	0.018	2.22	−0.20, 0.24
	TAAM_UB	0.019	0.019	2.29	−0.16, 0.28
	TAAM_IM	0.02	0.02	2.45	−0.21, 0.30

The methyl C–H bond length recommended by the Invariom database is longer by 0.032 Å than that from the UBDB database. The systematic differences of BCP properties due to diverse methyl C–H distances are also seen in the outcome of the TAAM_IM, TAAM_UB and THEOR refinements, but not in the M and M_{KRMM} refinements (averaged neutron distances), which are expected to give results similar to M_UB_{KRMM}.

The BCP properties of the C7=O2 bond are changed after either application of the multipole parameters from the databases in the M_UB, M_IM refinements, or after constraining the κ' parameters in M_{KRMM}, M_UB_{KRMM} or M_IM_{KRMM}. The values of C7=O2 $\rho(\text{BCP})$ and $|\Delta\rho(\text{BCP})|$ from these models are smaller than in the M model and become closer to the values from THEOR. This is mainly due to the refinement of the C8 κ' parameter in the M model, which attempts to describe the density smearing resulting from the disorder of the methyl group.

In general, it is evident that density values are systematically larger in experimental models (M, M_UB, M_IM, M_{KRMM}, M_UB_{KRMM} and M_IM_{KRMM}) than in theory (TAAM refinements and THEOR) – the values of $\rho(\text{BCP})$ from the multipole refinements are higher by about 0.1 e \AA^{-3} on average. This effect could be due to inappropriate deconvolution of thermal motion from static density described by the inflexible multipolar model, or experimental error.

There are also some discrepancies in $\rho(\text{BCP})$ of the C7=O2, C7–C8 and C1–N1 bonds between the TAAM_UB and TAAM_IM refinements, which can be easily correlated with the differences in the amide-group ED (Fig. 3, Figs. 4S and 6S in the supplementary material). In the case of $|\Delta\rho(\text{BCP})|$, the above difference is apparent only at the C7=O2 BCP.

5.2. ED – differential and deformation maps

The most pronounced differences in the ED description are observed between multipole refinements (M, M_UB, M_IM, M_{KRMM}, M_UB_{KRMM} and M_IM_{KRMM}) and theoretical models (THEOR, TAAM_UB, TAAM_IM), see Fig. 3. Experimental multipolar models include additional density of

about $0.1 \text{ e } \text{Å}^{-3}$ in the bond regions, which corresponds well to the observed discrepancies in $\rho(\text{BCP})$. We ascribe this rather to inaccuracy of the models or experimental errors than to the effect of disorder, because the effect is observed in the whole molecule.

The extra density around O atoms in the experimental models results from improper deconvolution of thermal motion from multipolar expansion of the ED. It is clearly seen

on the M_{KRMM} deformation maps (Fig. 4) that the C4–O1 bonding density points towards the lone electron pair region of the O atom rather than the nucleus. Such a feature is not seen in the deformation maps from theoretical models (TAAM_UB, TAAM_IM, THEOR). Evidently, TAAM_UB and TAAM_IM refinements lead to more correct O-atom ADPs. On the other hand, neither database takes into account intermolecular interactions, hence these models include less

ED around the O1 atom, by about $0.2 \text{ e } \text{Å}^{-3}$, and next to the N1 atom, by about $0.1 \text{ e } \text{Å}^{-3}$, with respect to THEOR. Unexpectedly, the differences have consequences not for the $\rho(\text{BCP})$ values, but only for $|\Delta\rho(\text{BCP})|$ (Fig. 2). These values correspond well with the values found for the interaction densities by Dittrich & Spackman (2007).

In the M, M_UB and M_IM models, in which κ' parameters for the non-H atoms were refined, multipole parameters for the O1 atom also attempt to describe the smeared methyl-group density, which is not the case for M_{KRMM} , M_{UBKRMM} or M_{IMKRMM} . This effect is clearly noticeable in considering the differences in the ED distribution in the M, M_UB and M_IM models. The M_UB and M_IM models with multipole populations fixed for the methyl group seem to have a higher level of ED around the O1 atom (Fig. 3, Figs. 3S and 6S in the supplementary material).

The different description of the methyl group between the Invariom and UBDB databases, especially in values of P_v , together with the electroneutrality constraint applied in the refinements, results in discrepancies in the whole-molecule ED as observed in Fig. 3(b) and (c).

The deformation maps from TAAM refinements vary noticeably at the positions of the nuclei, in which the TAAM_UB deformation maps show minima ($\sim -0.2 \text{ e } \text{Å}^{-3}$) whereas the TAAM_IM maps show maxima ($\sim 0.5 \text{ e } \text{Å}^{-3}$). It seems that in the THEOR model, the ED description at the positions of the nuclei deviates from the Invariom and

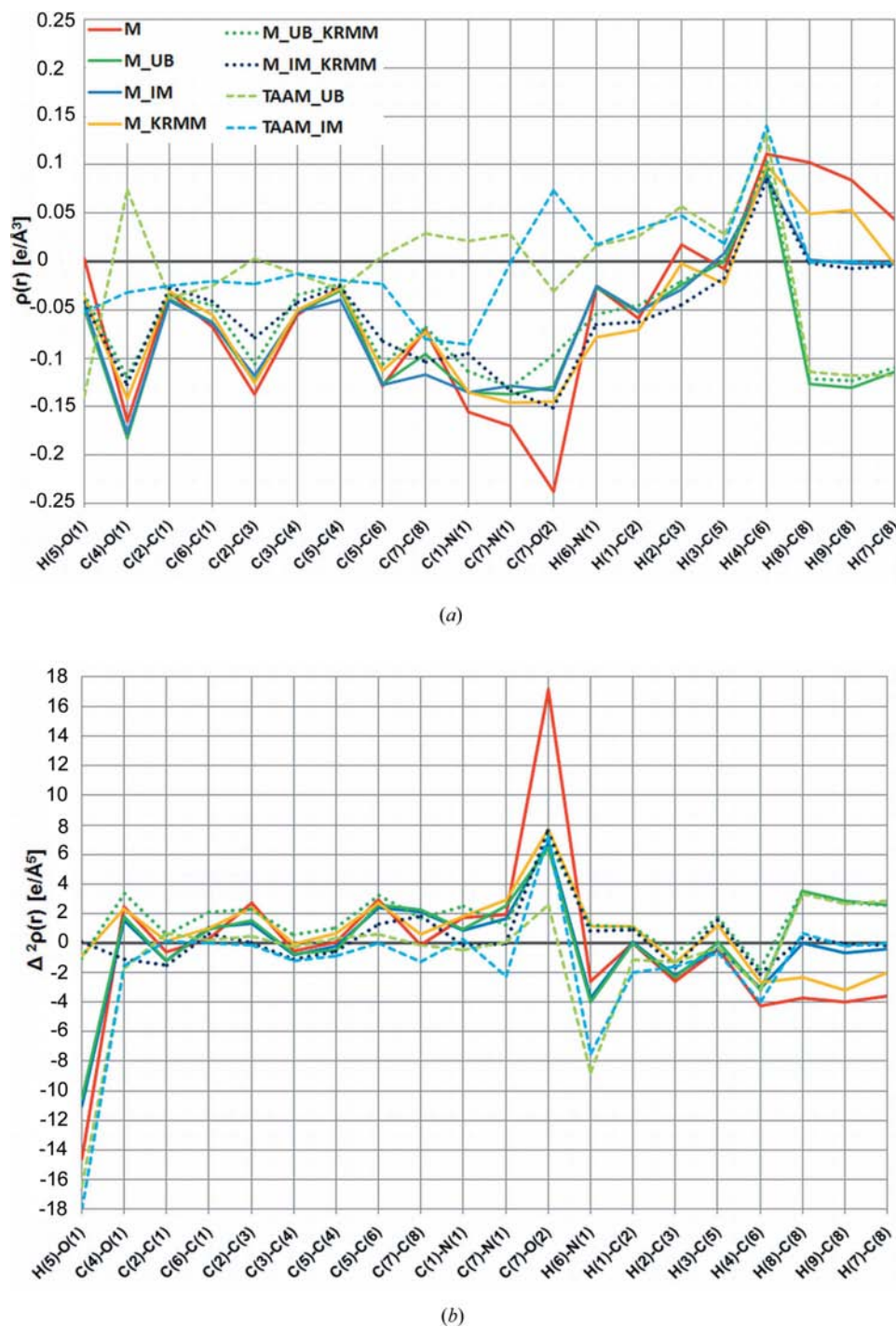


Figure 2

Differences in properties at the BCPs between THEOR and different models of refinement: (a) electron density ($\text{e } \text{Å}^{-3}$); (b) Laplacian of electron density ($\text{e } \text{Å}^{-5}$). The averaged standard deviations of $\rho(\text{BCP})$ and $|\rho(\text{BCP})|$ are 0.015 and 0.1 for X–X bonds, and 0.05 and 0.3 for X–H bonds, respectively.

multipole refinement description (Fig. 4) by about $1 \text{ e } \text{Å}^{-3}$. It is known that the currently used multipolar model is not flexible enough to describe properly the ED in the bond region and near the atom positions at the same time (Volkov *et al.*, 2000). The origin of this effect has been attributed to the limited flexibility of the single-exponential radial functions; thus the maxima might result from different basis sets used in the calculation of theoretical densities in the UBDB or Invariom databases, especially from the presence or absence of diffuse functions. Another possible reason for the different ED values at the atom positions is that the core orbitals are

excluded from the UBDB theoretical structure-factor calculations, whereas in the Invariom method all orbitals are used (see §1). Further studies are required to judge the physical significance of the differences and to choose the best approach to describing the nuclear region.

The ED around the amide group of paracetamol obtained from the Invariom model is asymmetric with respect to the C7=O2 and C7–C8 bonds – unlike in the case of the multipole refinements, the UBDB and THEOR models (see also in Fig. 2). The asymmetry might be caused by the choice of a particular local coordinate system for the C7 atom in the

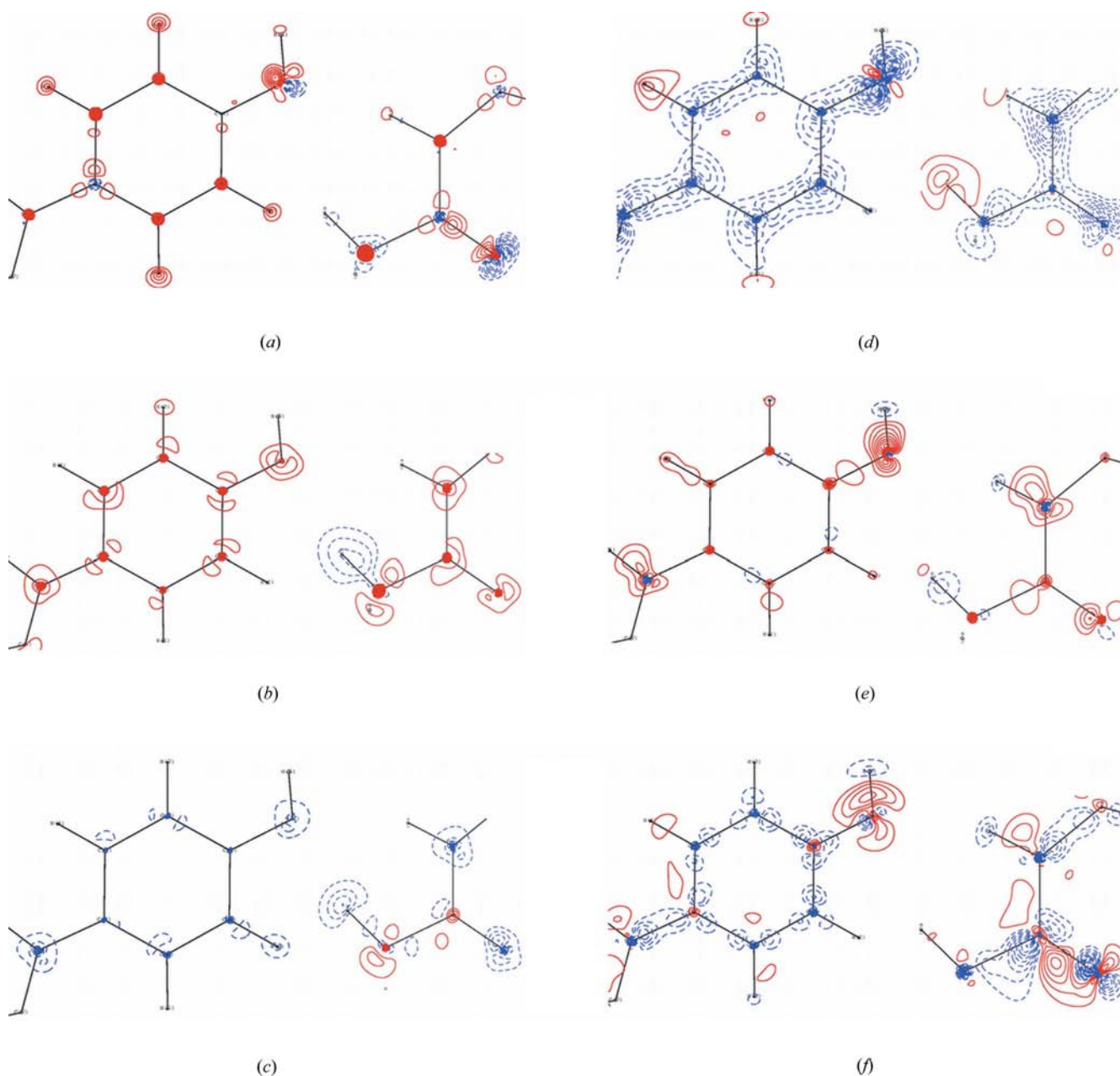


Figure 3 ED difference maps visualizing the discrepancy between the electron-density models in the plane of the phenyl ring (left) and in the plane of the C7=O2 bond (right): (a) $M - M_{KRMM}$; (b) $M_{KRMM} - M_{UB_{KRMM}}$; (c) $M_{KRMM} - M_{IM_{KRMM}}$; (d) $THEOR - M_{KRMM}$; (e) $THEOR - TAAM_{UB}$; (f) $THEOR - TAAM_{IM}$. Contour interval $0.05 \text{ e } \text{Å}^{-3}$, positive red, negative blue. The atom coordinates for the map-creation process were exactly the same for all maps.

Invariom database and at the same time by the difference in geometries between the model compound used to generate the Invariom values and the paracetamol molecule studied here.

Another difference between the TAAM_UB and TAAM_IM densities is visible around the phenyl C atoms (see Fig. 3e). Again, additional maxima can be caused by differences in the basis sets used in creating the databases.

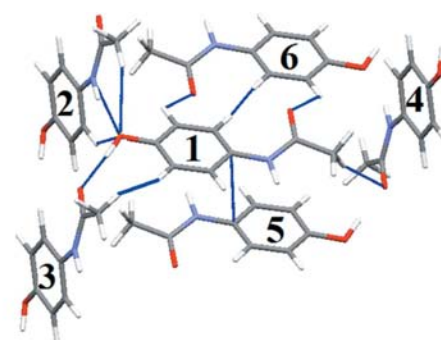
5.3. Electrostatic energy of interaction, electrostatic potential and dipole moment

The values of the electrostatic interaction energy for the dimers of paracetamol are given in Table 4 (see also Fig. 5) and Table 2S in the supplementary material. Problems with proper deconvolution of atom motions from the static charge density, especially in the methyl-group region, result in discrepancies in the values of the interaction energy between the M and M_IDP(H) models and other multipole refinements, and extreme energy values for the M_IDP(H) procedure, in which an isotropic model of motion for H atoms is used.

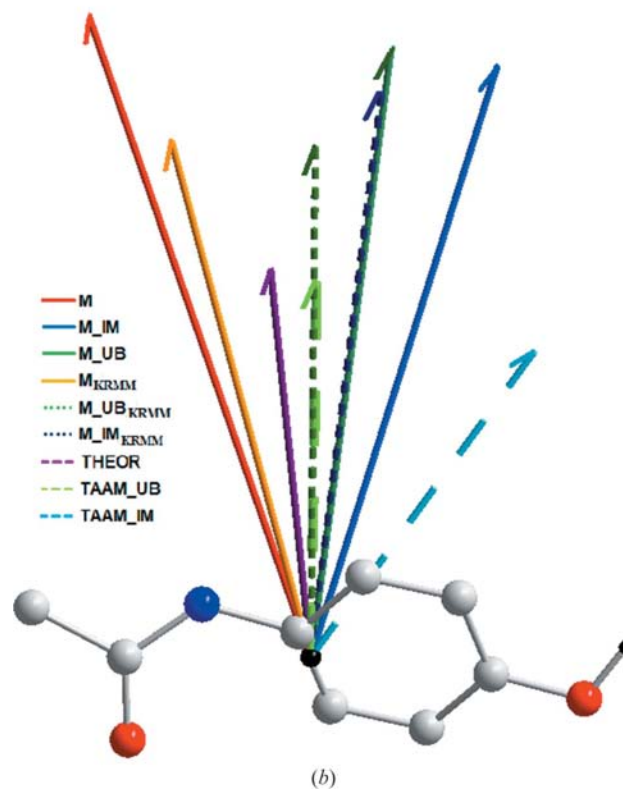
The M_UB and M_IM models with a restricted methyl group and the M_{KRMM}, M_UB_{KRMM} and M_IM_{KRMM} refinements with fixed κ' parameters give quite consistent values of electrostatic energy, except for the 1–3 interaction. It seems that restriction of the κ' parameters is required, since use of unrestricted multipole parameters for the nearest atoms could partially describe smeared ED from the disordered methyl group (Abramov *et al.*, 2000). Simultaneous use of the KRMM approach and modeling of the methyl group by the pseudoatoms from the databases brings the energy values for the 1–3 interaction closer to those from THEOR.

With the exception of the 1–3 interaction, there are systematic differences between the energies obtained from the

theoretical models (THEOR, TAAM_UB and TAAM_IM). THEOR gives higher energies than TAAM_UB, on average by 5 kJ mol⁻¹, while energies from TAAM_IM are lower than from TAAM_UB by about 7 kJ mol⁻¹. This may result from the UBDB approach excluding the core orbitals from the structure-factor calculation, from the differences in basis set used in theoretical calculations, or from the different geometries of the compounds used to generate the database. The UBDB databank is based on experimental geometries in which geometrical consequences of intermolecular interactions are to some extent included. Much higher energy differences than the average are found for the 1–3 (C–OH...C=O) interaction. The higher variations may be due to the ED being changed by intermolecular interactions, which are taken into account in periodic calculation, or the asym-



(a)



(b)

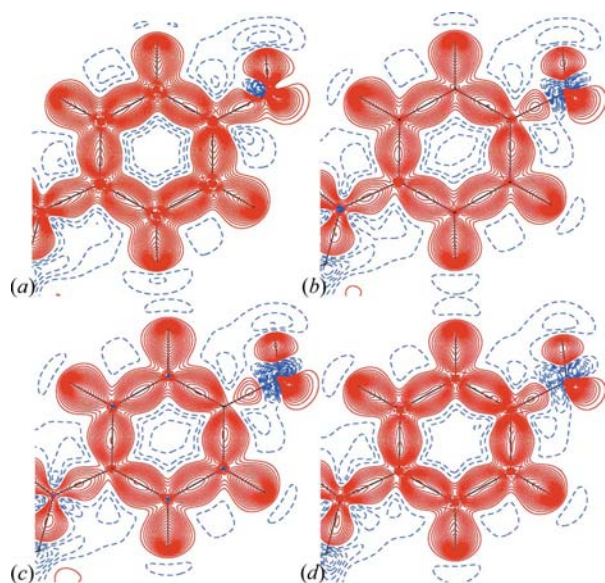


Figure 4

Deformation density maps in the plane of the phenyl ring: (a) M_{KRMM}; (b) THEOR; (c) TAAM_UB; (d) TAAM_IM. Contour interval 0.05 e Å⁻³, positive red; negative blue.

Figure 5

Visualization of: (a) interactions between paracetamol molecules; (b) dipole-moment vectors in the plane of the hydroxyl and amide group in paracetamol.

metric and slightly inadequate ED description of the carbonyl group in the TAAM_IM model.

Considering the electrostatic potential (see Figs. 6 and 7S in the supplementary material) mapped on the $0.0067 e \text{ \AA}^{-3}$ isosurface, the property often discussed in the context of intermolecular interactions, the M, M_{KRMM} and THEOR models are similar to one another and distinct from the other models. The modeling of the methyl group by pseudoatoms taken from databases does not improve the M_{KRMM} model. The transfer of inflexible methyl-group models from the databases ($M_{UB_{KRMM}}$ and $M_{IM_{KRMM}}$ refinements) has consequences for the electrostatic potential of the freely refined part of the molecule, since the values of electrostatic potential mapped on the isosurface are closer to zero for the whole molecule. These results also suggest that the electrostatic potential mapped on a single isodensity surface is not a sensitive probe for a total intermolecular electrostatic interaction.

The dipole-moment values depend strongly on the model and their magnitudes vary in the range 6–12 D (Fig. 5b). The experimental dipole-moment magnitude determined for paracetamol in dioxane, which is the average over a set of conformations, is 4 D (Lutsii *et al.*, 1963). The dipole-moment magnitudes obtained from both TAAM models (Table 4) agree with the earlier single-molecule calculation (6 D; Binev *et al.*, 1998) and with the value determined from the THEOR

Table 4

Electrostatic interaction energies (kJ mol^{-1}) for the dimers of paracetamol and molecular dipole moment (D).

Molecule 2 is at $[-0.5 + x, 0.5 - y, -0.5 + z]$; molecule 3 is at $[0.5 + x, 0.5 - y, -0.5 + z]$; molecule 4 is at $[-0.5 - x, 0.5 + y, -0.5 - z]$; molecule 5 is at $[-0.5 - x, 0.5 + y, -0.5 - z]$; and molecule 6 is at $[-1 - x, 1 - y, -1 - z]$ (see Fig. 5 for details).

Model	Interaction energy between molecules					Dipole moment
	1 and 2	1 and 3	1 and 4	1 and 5	1 and 6	
$M_{IDP(H)}$	-115	-45	-50	-57	-4	12
M	-83	-75	-37	-44	-8	10
M_{UB}	-68	-94	-20	-39	-8	9
M_{IM}	-65	-99	-18	-34	-9	9
M_{KRMM}	-64	-75	-23	-36	-10	8
$M_{UB_{KRMM}}$	-57	-83	-17	-36	-5	8
$M_{IM_{KRMM}}$	-63	-82	-20	-28	-9	8
THEOR	-48	-89	-19	-34	-8	6
TAAM_UB	-43	-63	-16	-30	-12	6
TAAM_IM	-34	-41	-8	-24	-6	6

model. The M_{KRMM} , $M_{UB_{KRMM}}$ and $M_{IM_{KRMM}}$ models lead to higher dipole-moment magnitudes than the theoretical values. Models with freely refined κ' parameters [M , $M_{IDP(H)}$] give unreliable dipole-moment magnitudes (Spackman *et al.*, 2007). We ascribe the dipole-moment enhancement to the ability of unrestricted multipole parameters to allow a partial description of smeared ED from the disordered methyl group (see Fig. 2a), thus leading to uncertainty in the partitioning of crystal space and to inadequate calculation of the dipole moment (Abramov *et al.*, 2000).

5.4. Shape of ADPs

Both TAAM refinements give much more reasonable ADPs than the IAM refinement (see Fig. 7 and Fig. 2S in the supplementary material) because they minimize bonding electron density and the contribution of systematic errors to the ADPs obtained (Volkov *et al.*, 2007; Dittrich *et al.*, 2008).

However, the differences in the ED distribution between the models lead to discrepancies in the ADPs. The deformation maps for the TAAM_IM and multipole refinements show maxima at the nuclei positions, hence the models give smaller ADPs than the TAAM_UB and TAAM_TH models, in which the maps have minima at the nuclei positions.

The O1 ADPs from M_{KRMM} are smaller in the O1–H5 direction and larger in the perpendicular direction (the lone-electron-pair direction) with respect to TAAM_TH. This confirms an earlier observation that deconvolution of the O1-atom thermal motion is not proper in all multipole refinements (M_{KRMM} , $M_{UB_{KRMM}}$, $M_{IM_{KRMM}}$). The TAAM_TH model includes information about crystal environment which is missing in both database approaches, therefore the shape of the O-atom ADPs differs among the TAAM refinements. The models of ED in the amide group vary between the TAAM_UB, TAAM_IM and TAAM_TH refinements, which produces deviations in the shape of the amide ADPs.

It was proposed that proper deconvolution of thermal motion and electron density in multipole refinement could be achieved by fixing the ADPs obtained from TAAM or high-

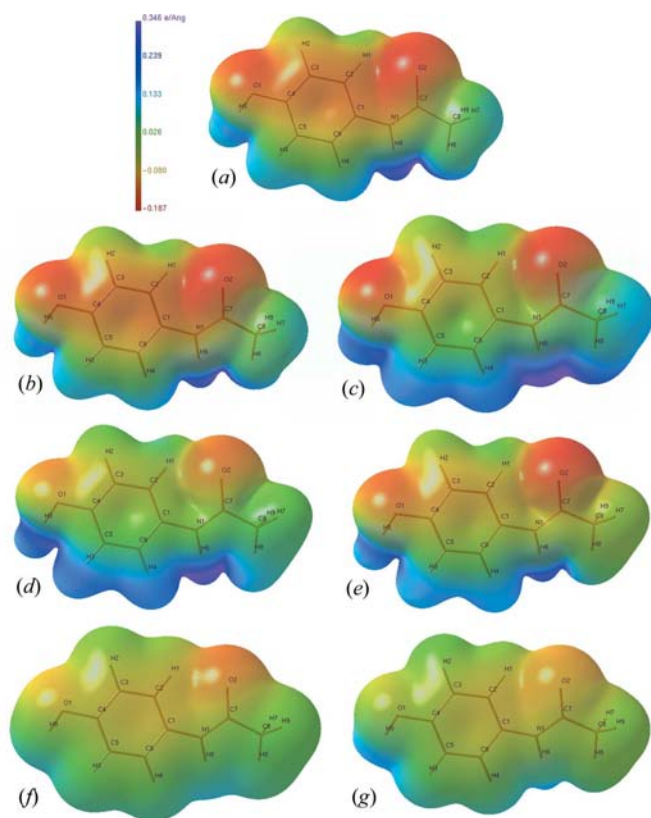


Figure 6

Electrostatic potential ($e \text{ \AA}^{-1}$) mapped on an ED isosurface at $\rho = 0.0067 e \text{ \AA}^{-3}$: (a) THEOR; (b) M; (c) M_{KRMM} ; (d) $M_{UB_{KRMM}}$; (e) $M_{IM_{KRMM}}$; (f) TAAM_UB; (g) TAAM_IM.

order refinement while multipole parameters are refined. However, the ADPs have a direct effect on the ED obtained in this way. We noted some systematic variations in EDs while performing multipole refinements on the ADPs obtained from the TAAM refinements. Before the databases are commonly used to refine ADPs, a careful discussion of the differences between them and possible errors associated with their use is needed.

6. Summary and conclusion

On the basis of high-resolution X-ray diffraction data measured for paracetamol crystals, different approaches to refining the experimental ED of the molecule, which contains a disordered methyl group, have been tested. The main objective of this work was to examine how reliable ED could be obtained for a molecule exhibiting such dynamic disorder. The refinement strategies tested did not include a precise model for the dynamic motion of the methyl group, which would require sophisticated calculations of an atomic probability density function (Dittrich *et al.*, 2009). Rather, we focused on the ordered part of the molecule and how it was influenced by different approximate models of static density of the methyl group. Firstly, we contrasted refinement with constrained κ' parameters (M_{KRMM} , $M_{\text{UB}_{\text{KRMM}}}$, $M_{\text{IM}_{\text{KRMM}}}$) with refinement with freely refined κ' parameters (M , M_{UB} , M_{IM}). Next, we analyzed the correctness of models in which the methyl group was represented by density built of pseudoatoms from the UBDB or the Invariom database (M_{UB} , M_{IM} , $M_{\text{UB}_{\text{KRMM}}}$, $M_{\text{IM}_{\text{KRMM}}}$) and multipole parameters for the remaining atoms were refined. By

comparing theoretical periodic calculations (THEOR) either with multipole refinements or with structural refinements (coordinates and ADPs) carried out in the presence of aspherical atoms transferred from the databases (TAAM), we have shown the limitations of the models and their influence on the ED properties, the electrostatic energies of interactions, the dipole moment and the ADPs.

The static electron density of the whole molecule is found to depend strongly on the model applied. The use of estimated ADPs for H atoms performs better than the use of isotropic displacement parameters, even for the disordered methyl H atoms. Restriction of κ' parameters in KRMM is essential in order to obtain values of the electrostatic interaction energy consistent with theoretical single-point periodic calculations. In such a strategy, there is a limited possibility that the multipole parameters of atoms with short contacts to the disordered group can simultaneously describe the methyl-group ED.

Simultaneous use of KRMM and restricted ED in the methyl group in the $M_{\text{UB}_{\text{KRMM}}}$ and $M_{\text{IM}_{\text{KRMM}}}$ models further corrects the electrostatic energy of interaction and the BCP properties. However, the $M_{\text{UB}_{\text{KRMM}}}$ and $M_{\text{IM}_{\text{KRMM}}}$ refinement procedures do not improve the electrostatic potential values mapped onto a $0.0067 \text{ e } \text{Å}^{-3}$ isodensity surface; we therefore recommend the above strategy, since the electrostatic potential mapped onto an isodensity surface seems not to be a proper probe for intermolecular electrostatic interactions.

The dipole-moment magnitudes obtained using database models are lower than from KRMM multipole refinements, and similar to those from theoretical periodic calculations.

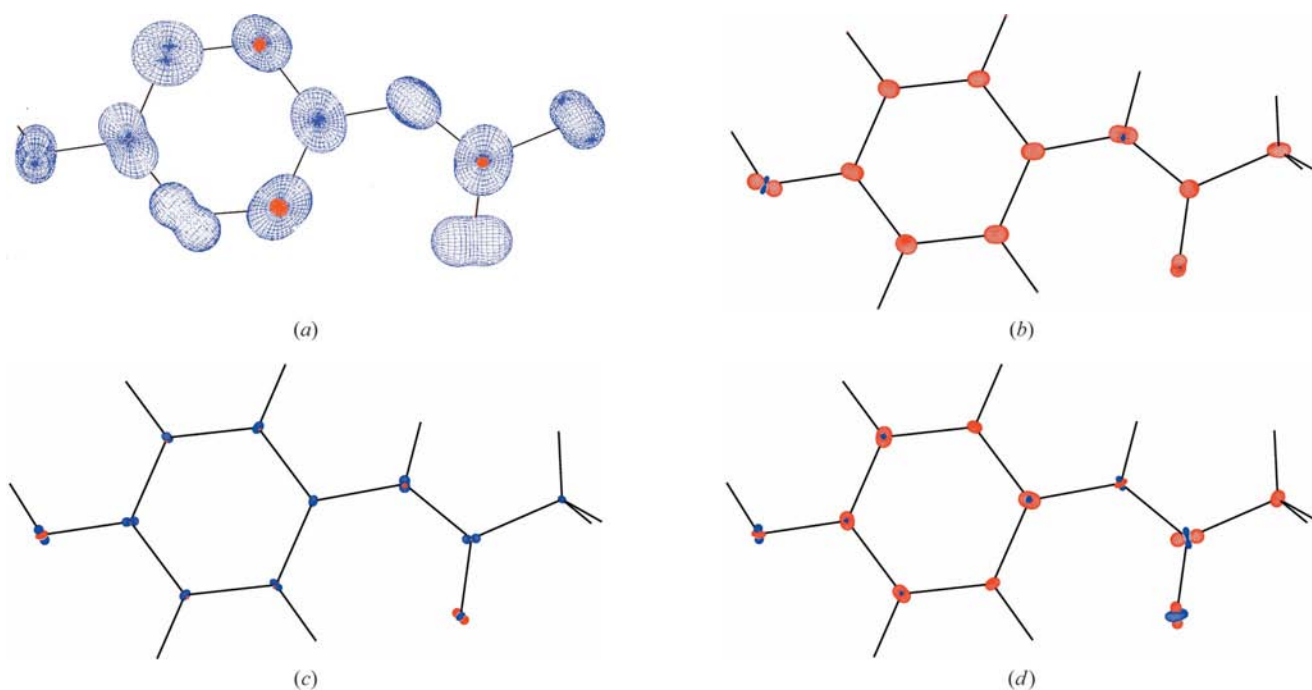


Figure 7

PEANUT representation (Hummel *et al.*, 1990) of the differences in anisotropic ADPs between (a) TAAM_TH and IAM; (b) TAAM_TH and M_{KRMM} ; (c) TAAM_TH and TAAM_UB; (d) TAAM_TH and TAAM_IM. An overestimation of the ADPs appears in blue. A scale of 10 was used for the representation of differences in root-mean-square deviation surfaces.

Comparison of the three TAAM refinements [with UBDB (TAAM_UB), Invariom (TAAM_IM) and periodic calculation parameters (TAAM_TH)] shows the influence of hydrogen bonding on the ED description of the hydroxyl and amide groups in paracetamol. Additional density is included in the THEOR model, therefore the electrostatic energy values are higher with respect to the other TAAM refinements and the shape of the ADPs is affected.

Diverse algorithms used to create databases result in differences in the ED at the positions of nuclei. This variation leads to larger ADPs obtained from TAAM_UB (as was found in TAAM_TH) than from TAAM_IM (as was found in the multipole refinement).

The X-ray measurements were accomplished at the Structural Research Laboratory, Warsaw University, Poland. KW thanks the Ministry of Science and Higher Education for financial support (grant 1 T09A 116 30). PMD would like to acknowledge support from a grant from Iceland, Liechtenstein and Norway through the EEA Financial Mechanism and the HOMING Programme from the Foundation for Polish Science (Edition 2007), and from grant 501/68-BW-175601. JMB and KW thank the Foundation for Polish Science for financial support within the 'Mistrz' programme.

References

- Abramov, Y. A., Volkov, A., Wu, G. & Coppens, P. (2000). *J. Phys. Chem. B*, **104**, 2183–2188.
- Allen, F. H. (2002). *Acta Cryst. B* **58**, 380–388.
- Allen, F. H., Kennard, O., Watson, D. G., Brammer, L., Orpen, A. G. & Taylor, R. (1987). *J. Chem. Soc. Perkin Trans. 2*, pp. S1–S19.
- Becke, A. D. J. (1993). *Chem. Phys.* **98**, 5648–5652.
- Binev, I. G., Boyadjieva, P. V. & Binev, Y. I. (1998). *J. Mol. Struct.* **447**, 235–246.
- Boldyreva, E. V., Shakhshneider, T. P., Vasilchenko, M. A., Ahsbahs, H. & Uchtmann, H. (2000). *Acta Cryst. B* **56**, 299–309.
- Bouhmaid, N., Bonhomme, F., Guillot, B., Jelsch, C. & Ghermani, N. E. (2009). *Acta Cryst. B* **65**, 363–374.
- Brock, C. P., Dunitz, J. D. & Hirshfeld, F. L. (1991). *Acta Cryst. B* **47**, 789–797.
- Bruker Nonius (2007). *APEXII-2008*. Version 1.0. Bruker Nonius, Delft, The Netherlands.
- Coppens, P. (2006). *International Tables for Crystallography*, Vol. B, 1st online ed., ch. 1.2, pp. 10–24. Chester: International Union of Crystallography. doi:10.1107/97809553602060000550.
- Dittrich, B., Hübschle, C. B., Luger, P. & Spackman, M. A. (2006). *Acta Cryst. D* **62**, 1325–1335.
- Dittrich, B., Hübschle, C. B., Messerschmidt, M., Kalinowski, R., Girnt, D. & Luger, P. (2005). *Acta Cryst. A* **61**, 314–320.
- Dittrich, B., Koritsánszky, T. & Luger, P. (2004). *Angew. Chem. Int. Ed.* **43**, 2718–2721.
- Dittrich, B., McKinnon, J. J. & Warren, J. E. (2008). *Acta Cryst. B* **64**, 750–759.
- Dittrich, B., Munshi, P. & Spackman, M. A. (2007). *Acta Cryst. B* **63**, 505–509.
- Dittrich, B. & Spackman, M. A. (2007). *Acta Cryst. A* **63**, 426–436.
- Dittrich, B., Strumpel, M., Schäfer, M., Spackman, M. A. & Koritsánszky, T. (2006). *Acta Cryst. A* **62**, 217–223.
- Dittrich, B., Warren, J. E., Fabbiani, F. P. A., Morgenroth, W. & Corry, B. (2009). *Phys. Chem. Chem. Phys.* doi:10.1039/b819157c.
- Domagała, S. & Jelsch, C. (2008). *J. Appl. Cryst.* **41**, 1140–1149.
- Dominiak, P. M., Volkov, A., Li, X., Messerschmidt, M. & Coppens, P. (2007). *J. Chem. Theory Comput.* **3**, 232–247.
- Dovesi, R., Saunders, V. R., Roetti, C., Orlando, R., Zicovich-Wilson, C. M., Pascale, F., Civalleri, B., Doll, K., Harrison, N. M., Bush, I. J., D'Arco, Ph. & Llunell, M. (2008). *CRYSTAL06 1.0*. Version 1_0_2. University of Turin, Italy.
- Flaig, R., Koritsánszky, T., Zobel, D. & Luger, P. (1998). *J. Am. Chem. Soc.* **120**, 2227–2238.
- Haisa, M., Kashino, S., Kawai, R. & Maeda, H. (1976). *Acta Cryst. B* **32**, 1283–1285.
- Haisa, M., Kashino, S. & Maeda, H. (1974). *Acta Cryst. B* **30**, 2510–2512.
- Hansen, N. K. & Coppens, P. (1978). *Acta Cryst. A* **34**, 909–921.
- Hariharan, P. C. & Pople, J. A. (1973). *Theor. Chim. Acta*, **28**, 213–222.
- Hoser, A. A., Dominiak, P. M. & Woźniak, K. (2009). *Acta Cryst. A* **65**, 300–311.
- Hübschle, C. B., Luger, P. & Dittrich, B. (2007). *J. Appl. Cryst.* **40**, 623–627.
- Hummel, W., Hauser, J. & Bürgi, H. B. (1990). *J. Mol. Graphics*, **8**, 214–218.
- Jelsch, C., Guillot, B., Lagoutte, A. & Lecomte, C. (2005). *J. Appl. Cryst.* **38**, 38–54.
- Johnas, S. K. J., Dittrich, B., Meents, A., Messerschmidt, M. & Weckert, E. F. (2009). *Acta Cryst. D* **65**, 284–293.
- Johnson, M. R., Prager, M., Grimm, H., Neumann, M. A., Kearley, G. J. & Wilson, C. C. (1999). *Chem. Phys.* **244**, 49–66.
- Koritsánszky, T. S. & Coppens, P. (2001). *Chem. Rev.* **101**, 1583–1627.
- Lee, C., Yang, W. & Parr, R. G. (1988). *Phys. Rev. B*, **37**, 785–789.
- Lutskii, A. E., Obukhova, E. M. & Kondratenko, B. P. (1963). *Zh. Fiz. Khim.* **37**, 1270.
- Madsen, A. Ø. (2006). *J. Appl. Cryst.* **39**, 757–758.
- Madsen, A. Ø., Sørensen, H. O., Flensburg, C., Stewart, R. F. & Larsen, S. (2004). *Acta Cryst. A* **60**, 550–561.
- Munshi, P. & Guru Row, T. N. (2006). *Cryst. Growth Des.* **6**, 708–718.
- Oddershede, J. & Larsen, S. (2004). *J. Phys. Chem. A*, **108**, 1057–1063.
- Pichon-Pesme, V., Jelsch, C., Guillot, B. & Lecomte, C. (2004). *Acta Cryst. A* **60**, 204–208.
- Pichon-Pesme, V., Lecomte, C. & Lachezar, H. (1995). *J. Phys. Chem.* **99**, 6242–6250.
- Pisani, C., Dovesi, R. & Roetti, C. (1988). *Lecture Notes in Chemistry*, Vol. 48. Heidelberg: Springer Verlag.
- Roversi, P. & Destro, R. (2004). *Chem. Phys. Lett.* **386**, 472–478.
- Sheldrick, G. M. (1996). *SADABS*. University of Göttingen, Germany.
- Sheldrick, G. M. (2008). *Acta Cryst. A* **64**, 112–122.
- Spackman, M. A. & Mitchell, A. S. (2001). *Phys. Chem. Chem. Phys.* **3**, 1518–1523.
- Spackman, M. A., Munshi, P. & Dittrich, B. (2007). *Chem. Phys. Chem.* **8**, 2051–2063.
- Volkov, A., Abramov, Y., Coppens, P. & Gatti, C. (2000). *Acta Cryst. A* **56**, 332–339.
- Volkov, A., Abramov, Y. A. & Coppens, P. (2001). *Acta Cryst. A* **57**, 272–282.
- Volkov, A., Koritsánszky, T., Li, X. & Coppens, P. (2004). *Acta Cryst. A* **60**, 638–639.
- Volkov, A., Li, X., Koritsánszky, T. S. & Coppens, P. J. (2004). *Phys. Chem. A*, **108**, 4283–4300.
- Volkov, A., Macchi, P., Farrugia, L. J., Gatti, C., Mallinson, P., Richter, T. & Koritsánszky, T. (2006). *XD2006*.
- Volkov, A., Messerschmidt, M. & Coppens, P. (2007). *Acta Cryst. D* **63**, 160–170.
- Whitten, A. E. & Spackman, M. A. (2006). *Acta Cryst. B* **62**, 875–888.
- Whitten, A. E., Turner, P., Klooster, W. T., Piltz, R. O. & Spackman, M. A. (2006). *J. Phys. Chem. A*, **110**, 8763–8776.
- Wilson, C. C. (1997). *Chem. Phys. Lett.* **280**, 531–534.